

Supporting Information

A Dinuclear Gold(I) Complex as a Novel Photoredox Catalyst for Light-Induced Atom Transfer Radical Polymerization

Frida Nzulu, Sofia Telitel, François Stoffelbach, Bernadette Graff, Fabrice Morlet-Savary, Jacques Lalevée, Louis Fensterbank,* Jean-Philippe Goddard,* Cyril Ollivier**

SUMMARY

I. General information	2
A. Chemicals	2
B. Irradiation Devices	2
C. Technical Characterizations	2
II. Preparation and characterization of [Au₂(dppm)₂]Cl₂ (1)	5
A. General preparation	5
B. NMR spectra	5
C. Cyclic voltammogram (CV) and Differential pulse voltammogram (DPV) of 1	7
D. Absorption spectrum of 1	8
E. Luminescence and absorption spectra of [Au₂]^{II*}	8
F. Characterization of ethyl α-bromophenylacetate (2)	9
1. Absorption spectrum of (2)	9
2. CV and DPV of (2)	9
G. Estimation of the free energy change ΔG⁰ between [Au₂]^{II*} and EBPA	10
H. Quench of [Au₂]^{II*} by oxygen	10
1. Steady State photolysis	10
2. Laser Flash Photolysis (LFP): [Au ₂]	12
III. Photo-ATRP of PMMA catalyzed by [Au₂(dppm)₂]Cl₂ (1)	12
A. General polymerization procedure	12
B. NMR spectrum	13
C. Comparison between photopolymerization in DCM and in DMF	13
D. General chain extension procedure	15
E. NMR spectrum	15
F. Mass Spectrometry study of PMMA	16
G. Atom Transfer Radical Addition (ATRA) experiment	18
IV. Photopolymerization in laminate	19
A. General photopolymerization procedure	19
1. Luminescence spectrum of the formulation after irradiation	20
2. Transmission Electron Microscopy (TEM)	21
3. X-ray Photoelectron Spectroscopy (XPS)	22

I. General information

A. Chemicals

Methyl methacrylate (MMA) (99% Aldrich) was washed with aqueous 5% NaOH then twice with distilled water, dried with MgSO_4 overnight then CaH_2 and distilled under reduced pressure. The distillate was stored in the fridge (4 °C). Benzyl methacrylate (BnMA) was purchased from Sigma-Aldrich and passed through a plug of basic alumina before use. Dichloromethane (DCM) was purchased from Sigma-Aldrich and distilled from CaH_2 . Dimethylformamide (DMF), ethyl α -bromophenylacetate and 2,2,3,3,4,4-heptafluorobutyl acrylate (HFBA) were purchased from Sigma-Aldrich and used as received. Trimethylolpropane triacrylate (TMPTA) was obtained from Sartomer and used as received. Acetonitrile (MeCN) HiPerSolv was purchased from VWR and used as received.

B. Irradiation Devices

The reaction mixture were exposed to 16 bulbs into Rayonet at 300 nm, 350 nm, 380 nm or 419 nm (30 watts/bulbs) which was purchased from Southern New England Ultraviolet Company.

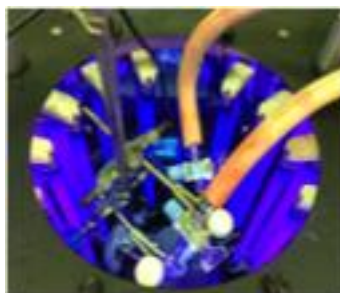


Figure 1- SI-2. Picture of the photopolymerization reaction placed in the Rayonet ($\lambda = 350 \text{ nm}$)

C. Technical Characterizations

Nuclear magnetic resonance: ^1H NMR spectra were recorded at 400 MHz and data are reported as follows: chemical shift in ppm from tetramethylsilane with the solvent as an internal standard (CDCl_3 δ 7.26 ppm, CD_2Cl_2 δ 5.32 ppm), multiplicity (s = singlet, d = doublet, t = triplet, q = quartet, m = multiplet, or overlap of non-equivalent resonances), integration, coupling constant if relevant. ^{13}C NMR spectra were recorded at 100 MHz and data are reported as follows: chemical shift in ppm from tetramethylsilane with the solvent as an internal standard (CDCl_3 δ 77.16 ppm, CD_2Cl_2 δ 54.00 ppm), integration if different from 1C, multiplicity regarding to the proton (C^{quat} , CH, CH_2 or CH_3). ^{31}P NMR spectra were recorded at 121 MHz and chemical shift are reported in ppm from phosphoric acid as an internal standard.

Infra-red (IR): IR spectra were measured using Tensor 27 (ATR diamond) Bruker spectrometer. IR data are reported as characteristic bands (cm^{-1}).

Cyclic voltammogram (CV): CV were recorded using Autolab PGSTAT 100, and were performed in acetonitrile solutions containing 0.1 M $[\text{N}(\text{n-Bu}_4)]\text{PF}_6$ supporting electrolyte at a glassy carbon working electrode, a KCl saturated calomel reference electrode, and a platinum wire as a counter electrode.

Size exclusion chromatography (SEC): The number-average molar masses (M_n), the weight-average molar masses (M_w), and the molar mass distributions ($D = M_w/M_n$) were determined by SEC with a calibration curve based on narrow polymethylmethacrylate (PMMA) standards (from Polymer Standard Services), using the RI and UV detector. Measurements were performed on two PL Gel Mixte C $5\mu\text{m}$ columns (7.5×300 mm; separation limits: 0.2 to 2000 $\text{kg}\cdot\text{mol}^{-1}$) maintained at 40°C coupled with a solvent and sample delivery module Viscotek GPCmax and 2 modular detectors: a differential refractive index (RI) detector Viscotek 3580 and a Diode Array UV Detector Shimadzu SPD20-AV. THF was used as the mobile phase at a flow rate of $1\text{ mL}\cdot\text{min}^{-1}$, toluene was used as a flow rate marker. All polymers were injected after two filtrations through a basic alumina plug and through a $0.20\ \mu\text{m}$ pore-size membrane. The OmniSEC 4.6.2 software was used for data acquisition and data analysis.

ESR experiments: ESR spin-trapping (ESR-ST) experiments were carried out using an X-Band EMX-plus spectrometer (Bruker Biospin). The radicals were produced at RT under a LED bulb exposure and trapped by phenyl-N-*t*-butylnitron (PBN) according to a procedure described in detail in [1].

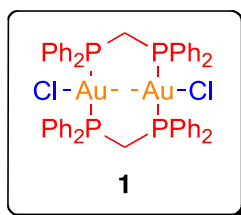
Laser Flash Photolysis: Nanosecond laser flash photolysis (LFP) experiments were carried out^[2] using a Qswitched nanosecond Nd/YAG laser ($\lambda_{\text{exc}} = 355\text{ nm}$, 9 ns pulses; energy reduced down to 10 mJ) from Continuum (Minilite) and an analyzing system consisting of a ceramic Xenon lamp, a monochromator, a fast photomultiplier and a transient digitizer (Luzchem LFP 212).

Contact Angle Analysis: Krüss drop shape analysis system DSA 100 is used for the measure of the contact angle. The support used is a glass slide with the polymer at the surface, a drop of water ($2\ \mu\text{L}$) is brought into contact with of polymer.

XPS analysis: X-ray photoelectron spectroscopy (XPS) spectra were recorded with a VG SCIENTA SES-2002 spectrometer equipped with a concentric hemispherical analyzer. The incident radiation used was generated by a monochromatic Al K α x-ray source (1486.6eV) operating at 420 W (14kV; 30mA). Photo-emitted electrons were collected at a take-off angle of 90° from the surface substrate, with electron detection in the constant analyser energy mode (FAT). Widescan spectrum signal was recorded with a pass energy of 500 eV; for the high resolution spectra (C1s, F1s, O1s, Au4f, Br3d, P2p, Cl2p and F1s), the pass energy was set to 100 eV. The analysed surface area was approximately 3 mm² and the base pressure in the analysis chamber during the experiment was about 10⁻⁹ mbar. Charging effects on these isolating samples were compensated by using of a Flood Gun. The spectrometer energy scale was calibrated using the Ag 3d^{5/2}, Au 4f^{7/2} and Cu 2p^{3/2} core level peaks, set respectively at binding energies of 368.2, 84.0 and 932.6 eV. Spectra were subjected to a Shirley baseline and peak fitting was made with mixed Gaussian-Lorentzian components with equal full-width-at-half-maximum (FWHM) using CASAXPS version 2.3.17 software. The surface composition expressed in atom% was determined using integrated peak areas of each component and took into account the transmission factor of the spectrometer, the mean free path and the Scofield sensitivity factors of each atom. All the binding energies (BE) are referenced to the aliphatic carbon C1s - (CH_x)- at 285.0 eV and given with a precision of 0.1eV.

MALDI-TOF and ESI-TOF mass spectrometry (MS) conditions: Mass spectra were recorded by Electrospray Ionization time-of-flight (ESI-TOF) mass spectrometry using a Bruker micrOTOF mass spectrometer (electrospray source, Agilent ESI-L Low Concentration Tuning Mix as reference) and a matrix-assisted laser desorption and ionization time-of-flight (MALDI-TOF) mass spectrometry using a Bruker autoflex III smartbeam mass spectrometer, equipped with a laser that produces pulses at 337 nm using *trans*-2-[3-(4-tert-butylphenyl)-2-methyl-2-propenylidene]malononitrile (DCTB) as a matrix and NaI as a cationizing agent. Spectra were recorded in linear mode at an accelerating potential of 20 kV. Samples were prepared by dissolving the polymer in THF at a concentration of 2-5 mg.mL⁻¹. A 10 μ L aliquot of this solution was mixed with 20 μ L of matrix solution and 10 μ L of NaI solution (both at 20 mg.mL⁻¹ in THF). Standard (polystyrene of known structure, $M_n = 1120$ g.mol⁻¹ purchased from Polymer Standards Service) was used to calibrate the mass scale.

II. Preparation and characterization of $[\text{Au}_2(\text{dppm})_2]\text{Cl}_2$ (**1**)



A. General preparation

$[\text{Au}_2(\text{dppm})_2]\text{Cl}_2$ **1** was prepared according to the Barriault's procedure.[3]

In a solution of chloro(dimethylsulfide)gold(I) (117 mg, 0.4 mmol) in dichloromethane (10 mL), bis(diphenylphosphino)methane was added (154 mg, 0.4 mmol). The reaction mixture was stirred for 1 h at room temperature and then concentrated to afford 1 mL. The complex was crashed out in diethyl ether (10 mL) and isolated by filtration as a white solid (215 mg, 43%). ^1H NMR (400 MHz, CD_2Cl_2): δ 7.91-7.89 (m, 16H), 7.48 (t, $J = 8$ Hz, 8H), 7.40 (t, $J = 8$ Hz, 16H), 4.72 (m, 4H), 1.97 (s, 3.76H, H_2O). ^{13}C NMR (100 MHz, CD_2Cl_2): δ 134.2 (m, 16C), 132.5 (s, 8C), 129.6 (s, 16C), 128.6 (m, 8C), 30.01 (m, 2C). ^{31}P NMR (121 MHz, CD_2Cl_2): δ 32.98 (s, 4P).

B. NMR spectra

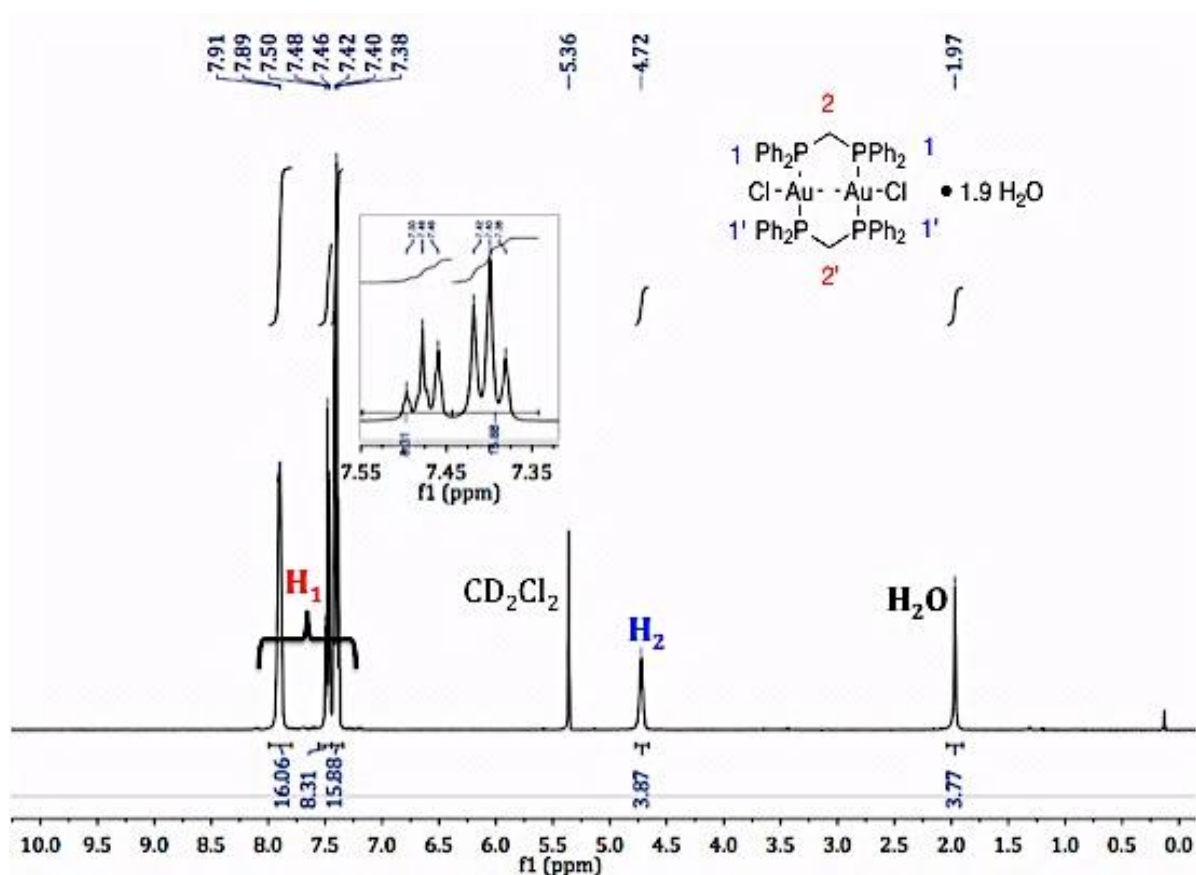


Figure 2-SI-5. ^1H (CD_2Cl_2 , 400 MHz).

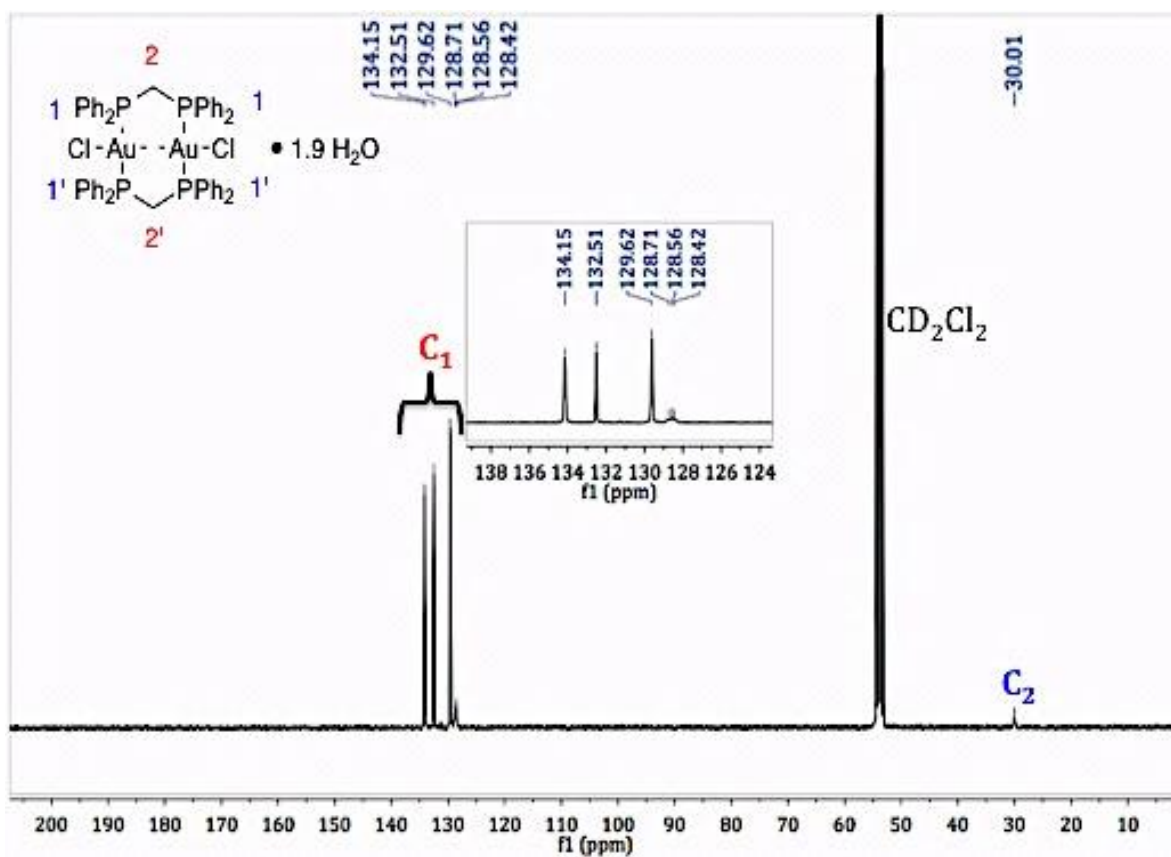


Figure 3-SI-6. ^{13}C (CD_2Cl_2 , 100 MHz).

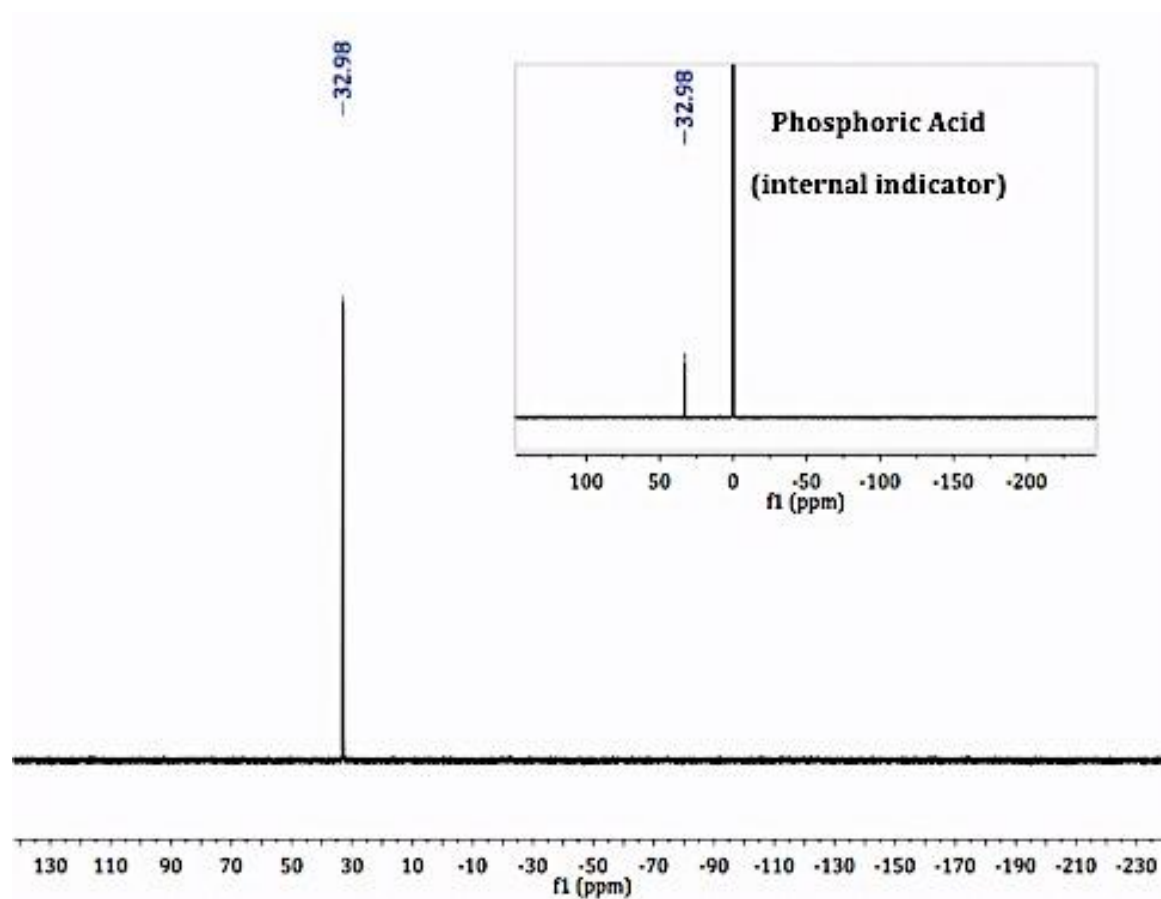


Figure 4-SI-6. ^{31}P (CD_2Cl_2 , 121 MHz).

C. Cyclic voltammogram (CV) and Differential pulse voltammogram (DPV) of 1

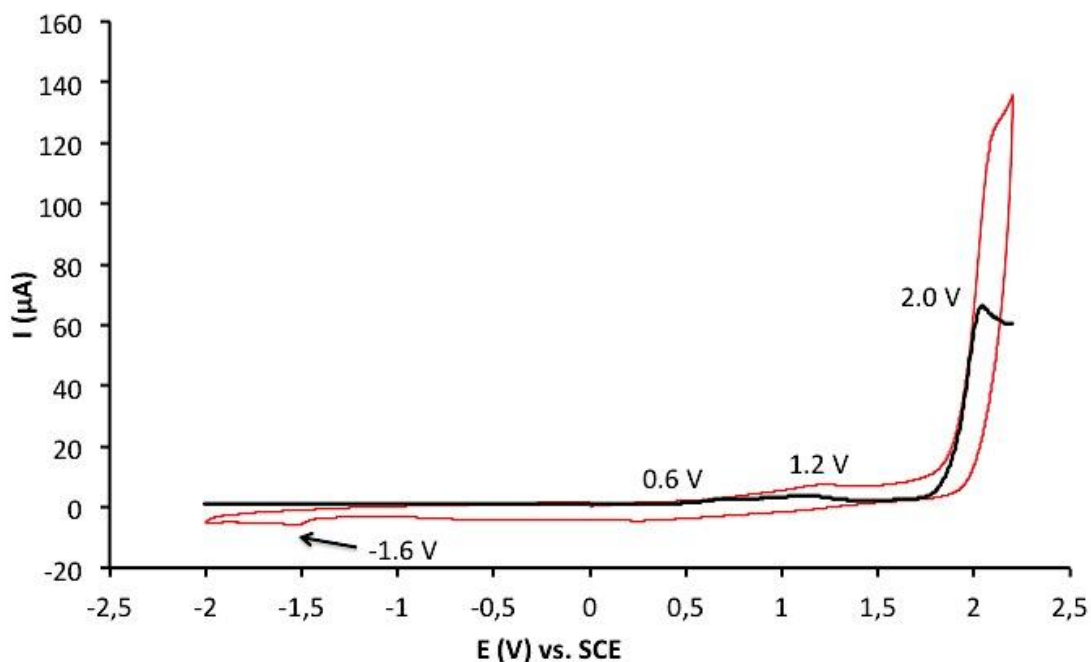


Figure 5-SI-7. Cyclic voltammogram (CV) of **1** (0.1 mM) (red line) with a rate of $100 \text{ mV}\cdot\text{s}^{-1}$ in MeCN with 100 mM of Bu_4NPF_6 as electrolyte. Differential pulse voltammogram (DPV) of **1** (0.1 mM) (black line) with a rate of $10 \text{ mV}\cdot\text{s}^{-1}$ in MeCN with 100 mM of Bu_4NPF_6 as electrolyte. CV and DPV showed one reduction potential at -1.6 V and three oxidation potentials at 0.6 V, 1.2 V and 2.0 V. The first wave at +0.6 V is assigned to Au^{I} metal-centered oxidation process.

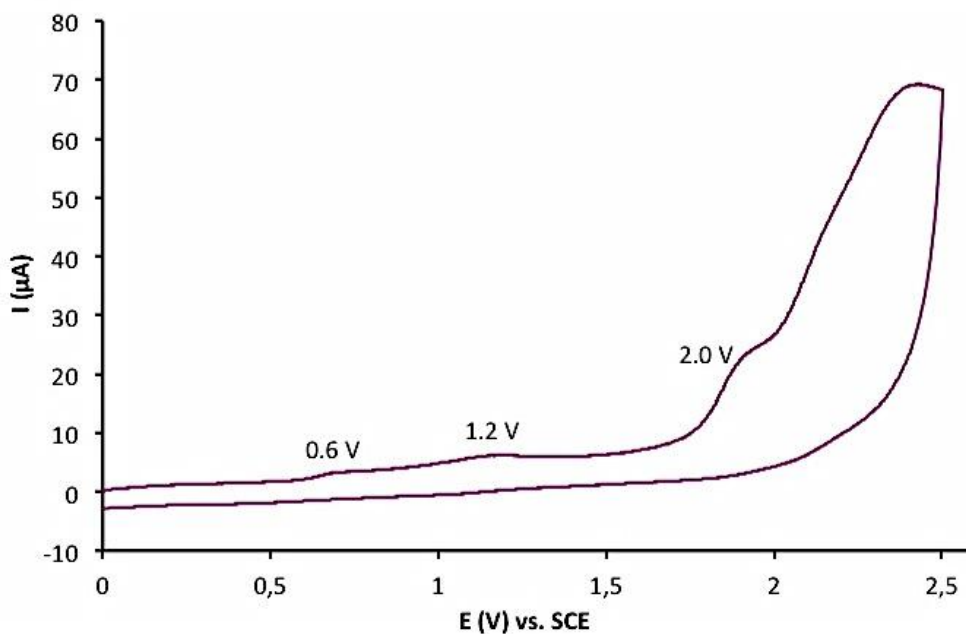


Figure 6-SI-7. Cyclic voltammogram (CV) of **1** (0.1 mM) (purple line) with a rate of $50 \text{ mV}\cdot\text{s}^{-1}$ in MeCN with 100 mM of Bu_4NPF_6 as electrolyte. CV showed one reduction potential at -1.6 V and three oxidation potentials at 0.6 V, 1.2 V and 2.0 V.

D. Absorption spectrum of 1

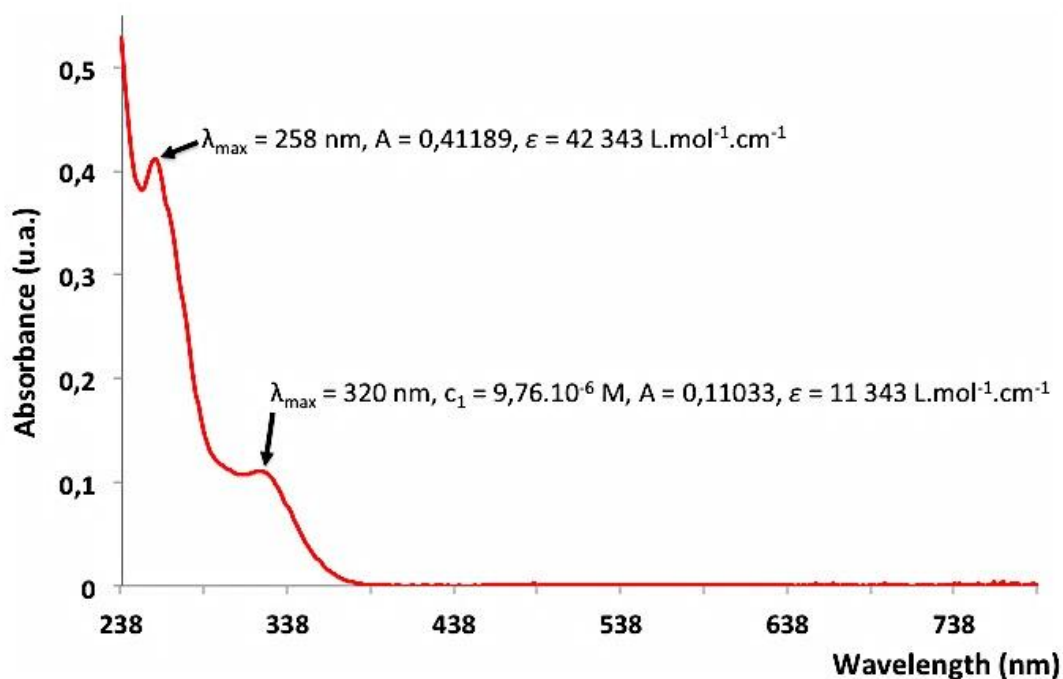


Figure 7-SI-8. Absorption spectrum of 1 ($9.76 \cdot 10^{-6}$ M in 3 mL of DCM) from 230 to 800 nm.

E. Luminescence and absorption spectra of $[\text{Au}_2]^{II*}$

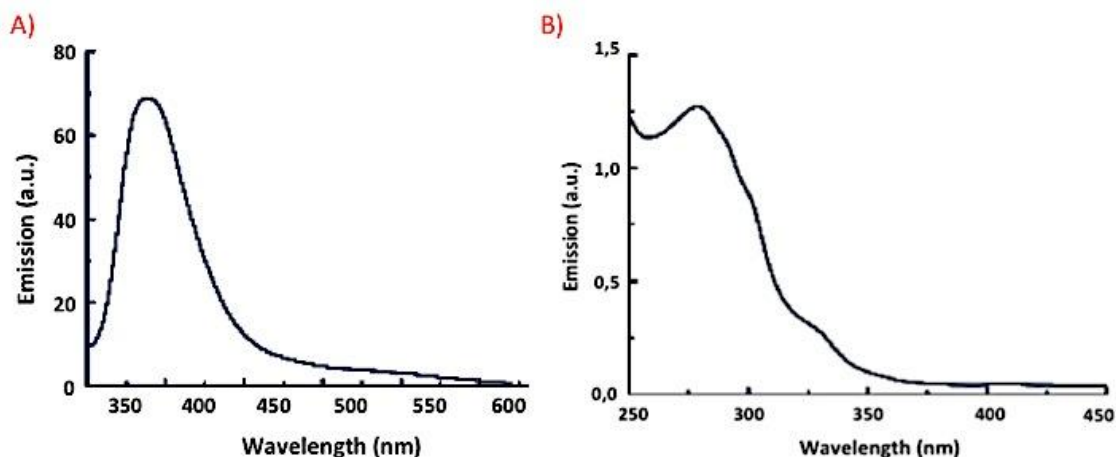


Figure 8-SI-8. A) $[\text{Au}_2]^{II*}$ ($7.5 \cdot 10^{-4}$ M in 3 mL of DCM) phosphorescence spectra recorded with an excitation wavelength 320 nm (the maximum absorption wavelength of 1). B) Absorption spectra of $[\text{Au}_2]^{II*}$ ($7.5 \cdot 10^{-4}$ M in 3 mL of DCM) recorded with an excitation at 350 nm. The long-wavelength band of low intensity centered at ~ 320 nm is assigned to a MLCT transition (See Fig 12-SI-11)

F. Characterization of ethyl α -bromophenylacetate (2)

1. Absorption spectrum of (2)

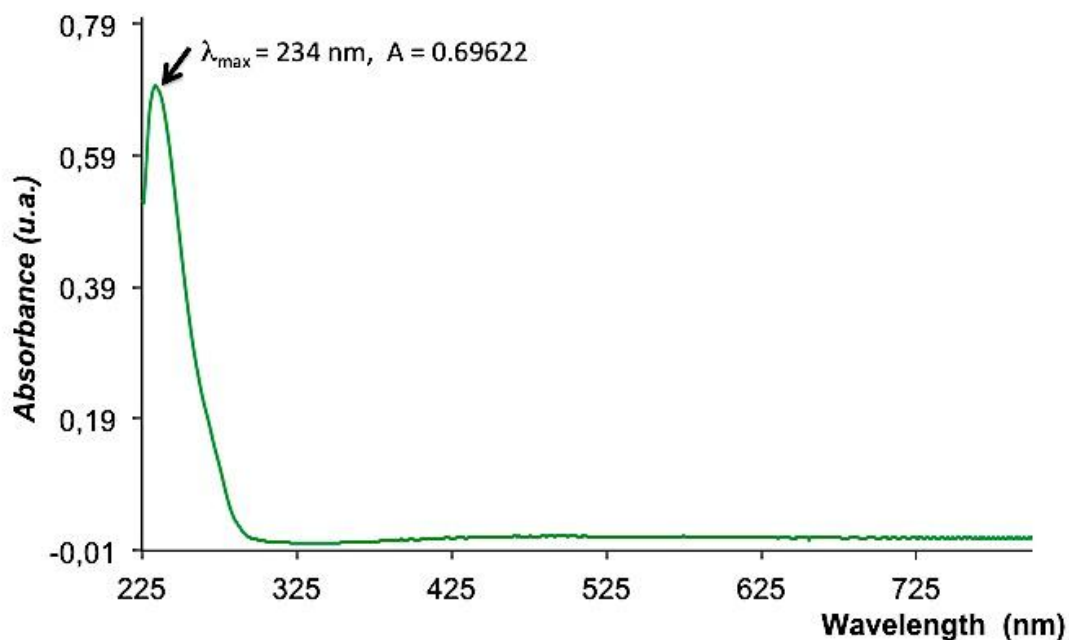


Figure 9-SI-9. Absorption spectrum of [EBPA] in DCM ($2.3 \cdot 10^{-4} \text{ M}$ in 3 mL of DCM) from 225 to 800 nm.

2. CV and DPV of (2)

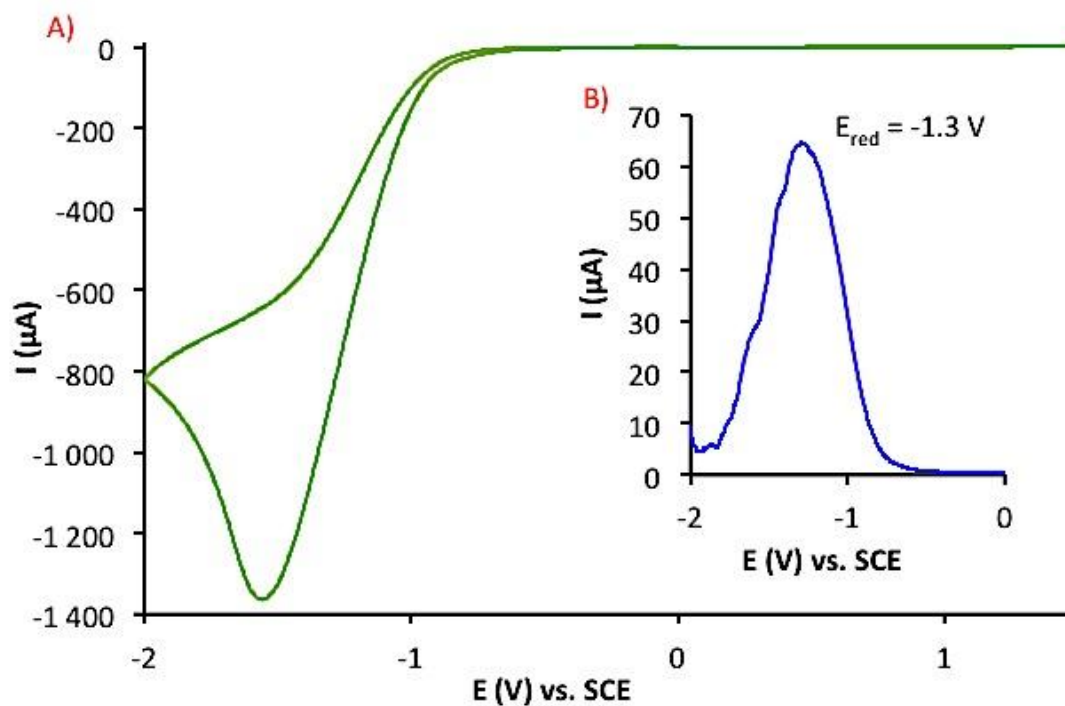
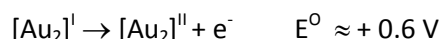


Figure 10-SI-9. A) Cyclic voltammogram (CV) of EBPA (2) (0.1 mM) with a rate of $100 \text{ mV}\cdot\text{s}^{-1}$ in MeCN with 100 mM of Bu_4NPF_6 as electrolyte. B) Differential pulse voltammogram (DPV) of 2 (0.1 mM) with a rate of $10 \text{ mV}\cdot\text{s}^{-1}$ in MeCN. DPV shows one reduction potential at -1.3 V .

G. Estimation of the free energy change ΔG^0 between $[\text{Au}_2]^{\text{II}*}$ and EBPA

The oxidation potential for the ground-state $[\text{Au}_2]^{\text{II}}$ can be obtained by electrochemical experiments. **1** shows three irreversible oxidation waves that appeared at +0.6 V, +1.2 V and +2.0 V vs S.C.E. The first wave is assigned to $[\text{Au}_2]^{\text{I}}$ metal-centered oxidation process:



The free energy change ΔG^0 for an electron transfer between **1** and EBPA (**2**) can be calculated from the classical Rehm-Weller equation - eq. 1, where E_{ox} , E_{red} , ${}^*E_{\text{exp}}$ (eq. 2) and C are the oxidation potential of **1**, the reduction potential of **2** ($E_{\text{red}} = -1.3 \text{ V}$), the excited singlet (or triplet) state energy of **1**, and the electrostatic interaction energy for the initially formed ion pair, generally considered as negligible in polar solvents - from the $[\text{Au}_2]^{\text{II}*}$ phosphorescence spectrum:

$$\Delta G^0 = E_{\text{ox}} - E_{\text{red}} - {}^*E_{\text{exp}} + C \quad (\text{eq. 1})$$

$${}^*E_{\text{exp}} \approx hc/\Delta\lambda_{\text{em/abs}} \quad (\text{eq. 2})$$

Using the average of the high energy side of the phosphorescence and absorption band $\Delta\lambda_{\text{em/abs}}$, the excited-state energy can be estimated to be ${}^*E_{\text{exp}} \approx 1240/((390+320)/2) \approx 3.5 \text{ eV}$, and the free energy change to be $\Delta G^0 \approx 0.6 + 1.3 - 3.5 \approx -1.6 \text{ eV}$.

H. Quench of $[\text{Au}_2]^{\text{II}*}$ by oxygen

1. Steady State photolysis

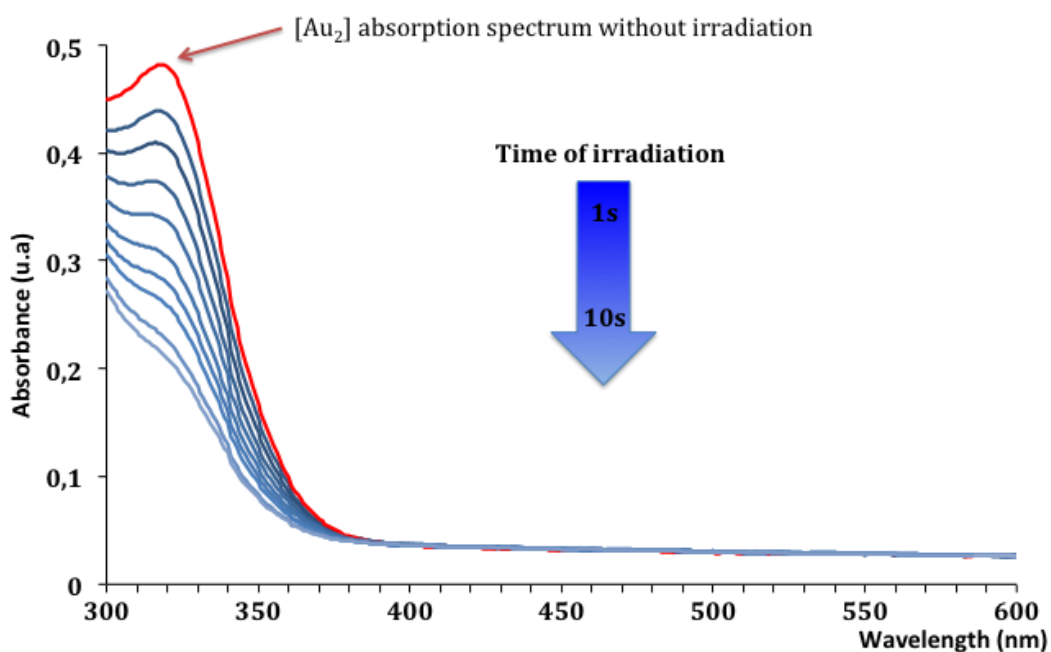


Figure 11-SI-10- At 20% of intensity. $[\text{Au}_2] = 3 \cdot 10^{-4} \text{ M}$ in 3 mL of DCM. If 10 s of irradiation is conducted in one shot complete consumption of $[\text{Au}_2]^{\text{II}*}$ is observed. ($[\text{Au}_2] = 1.5 \cdot 10^{-4} \text{ M}$ in 3 mL of DCM).

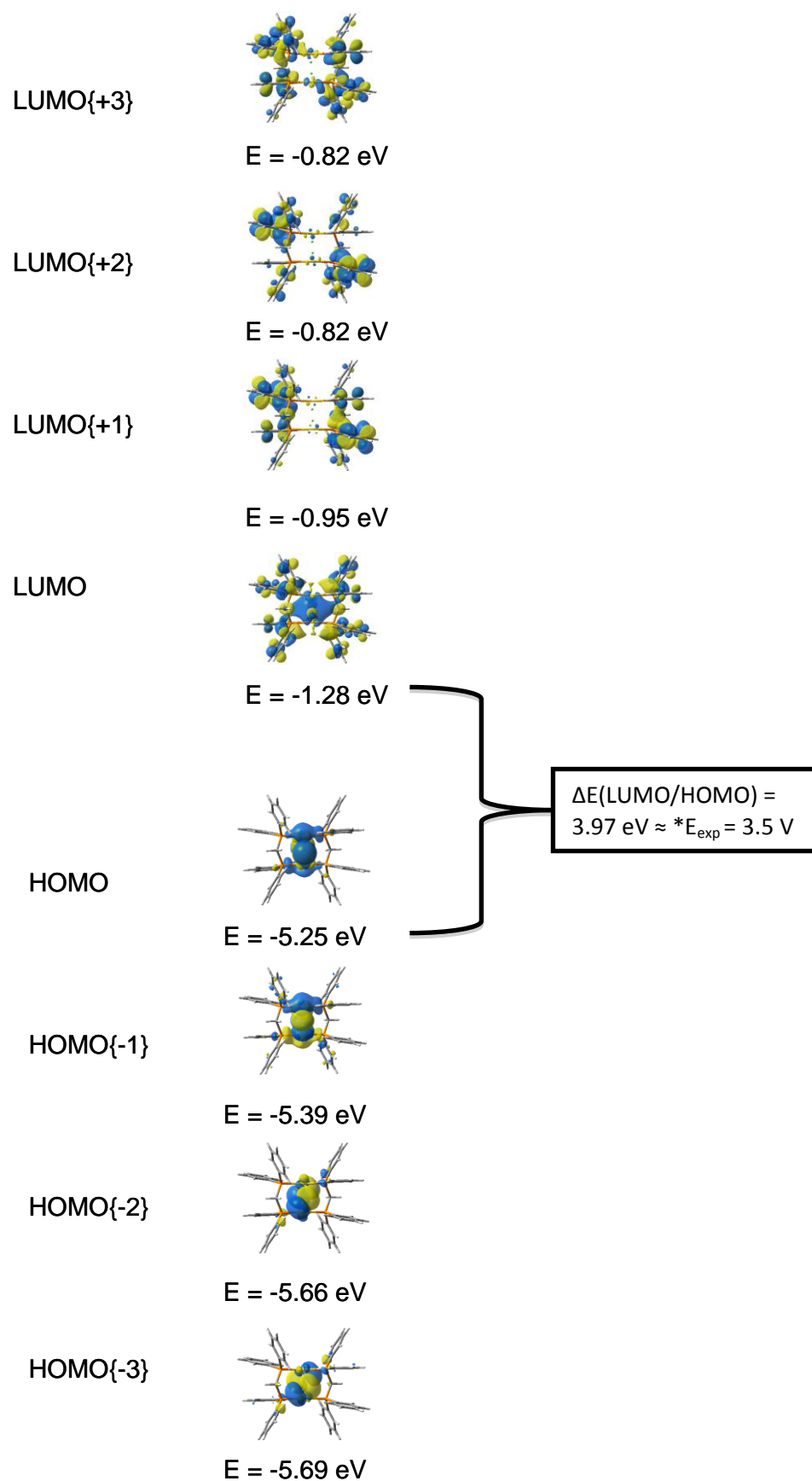
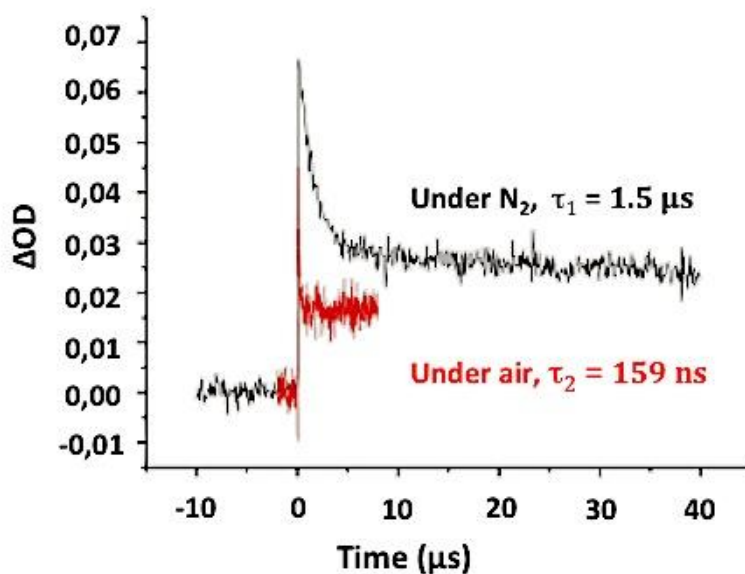


Figure 12-SI-11. Frontier molecular orbitals for the optimized geometry of the complex. The geometry has been optimized at B3LYP/LANL2DZ level from the X-Ray experimental structure as starting point.

2. Laser Flash Photolysis (LFP): [Au₂]



Rate constant photolysis of [Au₂]^{II*} by oxygen:

$$k(\text{Au}_2^*/\text{O}_2) = \tau_2/[\text{O}_2] = 2.5 \cdot 10^9 \text{ M}^{-1} \cdot \text{s}^{-1}$$

Figure 13-SI-12. Laser repetition frequency 10 Hz (10 pulsations/seconds). [Au₂] = 9.5 · 10⁻⁴ M in 3 mL of DCM spectroscopic quality (cells in quartz). [O₂] = 2.2 · 10⁻³ M in 3 mL of DCM (Handbook of Photochemistry).

III. Photo-ATRP of PMMA catalyzed by [Au₂(dppm)₂]Cl₂ (1)

A. General polymerization procedure

In a schlenk charged with a solution of complex **1** 4.2 · 10⁻³ M in DCM (or DMF) (61 μL, 0.0125 eq.), a solution of MMA 2.08 M in DCM (or DMF) (1.2 mL, 500 eq.) and DCM (or DMF) (4 mL) were added. The reaction mixture was degassed by freeze-pump-thaw three times. After covering the schlenk with aluminum foil, a solution of ethyl α-bromophenylacetate 2.3 · 10⁻¹ M in DCM (or DMF) (99 μL, 1 eq.) was added via syringe. After 24 h stirred in Rayonet under light exposure (λ = 300, 350, 380 or 419 nm), the reaction mixture was covered with aluminum foil and transferred via syringe to a round bottom flask containing a cold mixture of methanol (158 mL). The white precipitate was filtered over filter paper under water pump vacuum and collected with DCM to give the desired product. Aliquots from the reaction mixture were removed at different time to give the conversion of MMA using gravimetric method and analyzed by SEC to give polymer characteristic (*M_n*, *M_w*, *M_w/M_n*). *M_{n,exp}* = 24.7 kg·mol⁻¹, *M_w/M_n* = 1.62 (results obtained in DCM). ¹H NMR (300 MHz, CD₂Cl₂): δ 3.60 (s, 3H), 2.08-1.82 (m, 1.91H), 1.47 (m, 0.15H), 1.21 (m, 0.08H), 1.01 (s, 0.84H), 0.84 (bs, 2.07H). IR (neat): ν 2995, 2950, 1722, 1486, 1450, 1433, 1274, 1240, 1192, 1147, 993, 955, 749, 710, 676 cm⁻¹.

B. NMR spectrum

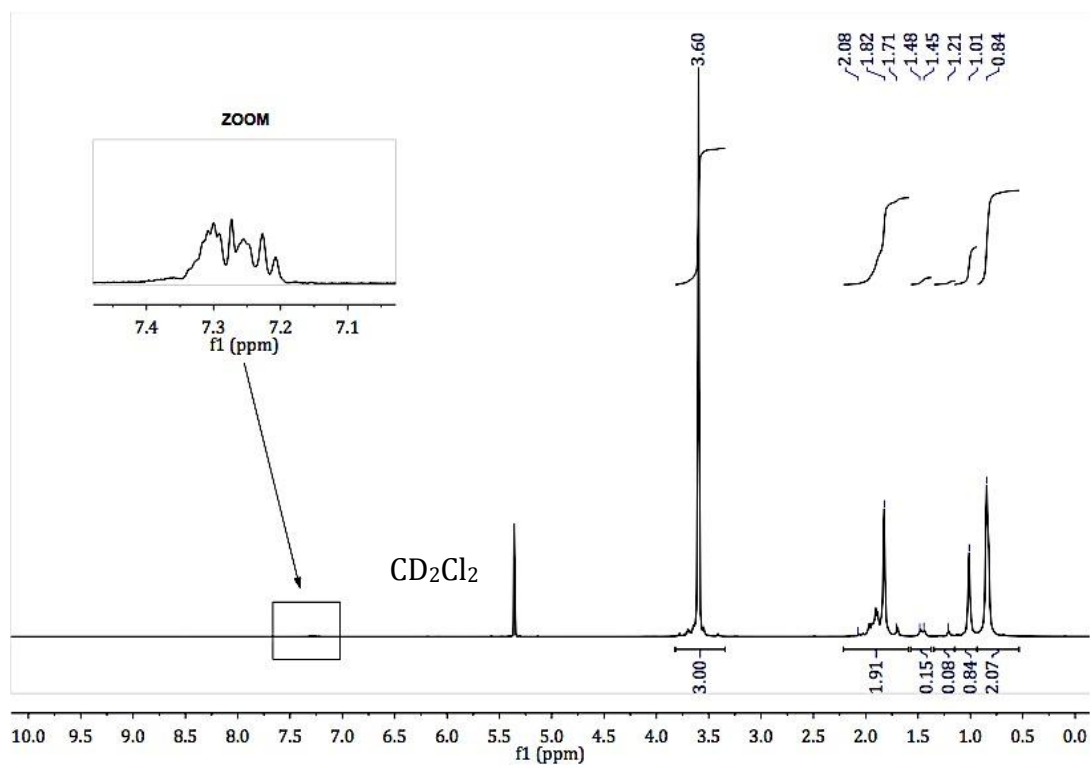


Figure 14-SI-13. ^1H (CD_2Cl_2 , 400 MHz).

C. Comparison between photopolymerization in DCM and in DMF

Reaction	Time (h)	p (%)	DP_n	$M_{n,th}$ ($\text{kg}\cdot\text{mol}^{-1}$)	$M_{n,exp}$ ($\text{kg}\cdot\text{mol}^{-1}$)	\bar{D}	$\text{Ln}(1/(1-p))$
	0	0	0	243.1		-	0
1	2	24	121	12.4	22.0	1.67	0.3
2	5	27	137	14.0	23.8	1.45	0.3
3	14	58	290	29.3	27.9	1.67	0.9
4	24	75	372	37.5	34.0	1.67	1.4

Table 1- SI-13. Photopolymerization in DMF, 350 nm, rt, $[\text{Au}_2]/\text{EBPA}/\text{MMA}$, 0.0125/1/500.

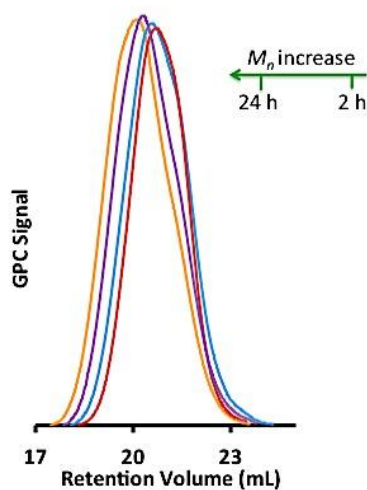


Figure 15-SI-13. Evolution of molecular weight during synthesis of PMMA-Br in DMF

Reaction	Time (h)	p (%)	DPn	$M_{n,th}$ ($\text{kg}\cdot\text{mol}^{-1}$)	$M_{n,exp}$ ($\text{kg}\cdot\text{mol}^{-1}$)	\bar{D}	$\ln(1/(1-p))$
	0	0	0	243.1		-	0,0
1	2	24	120	12.2	12.8	200	0,3
2	4	27	136	13.9	13.5	1.26	0,3
3	24	55	276	27.8	24.7	1.62	0,8

Table 2- SI-14. Photopolymerization in DCM, 350 nm, rt, $[\text{Au}_2]/\text{EBPA}/\text{MMA}$, 0.0125/1/500.

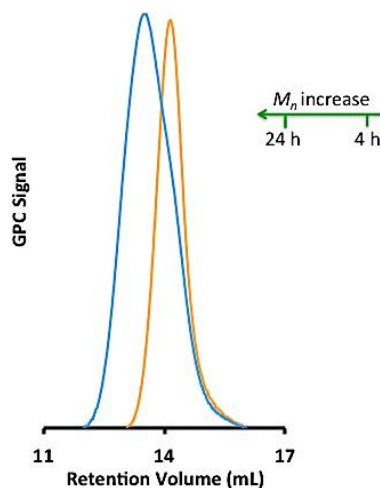


Figure 16-SI-14. Evolution of molecular weight during synthesis of PMMA-Br in DCM.

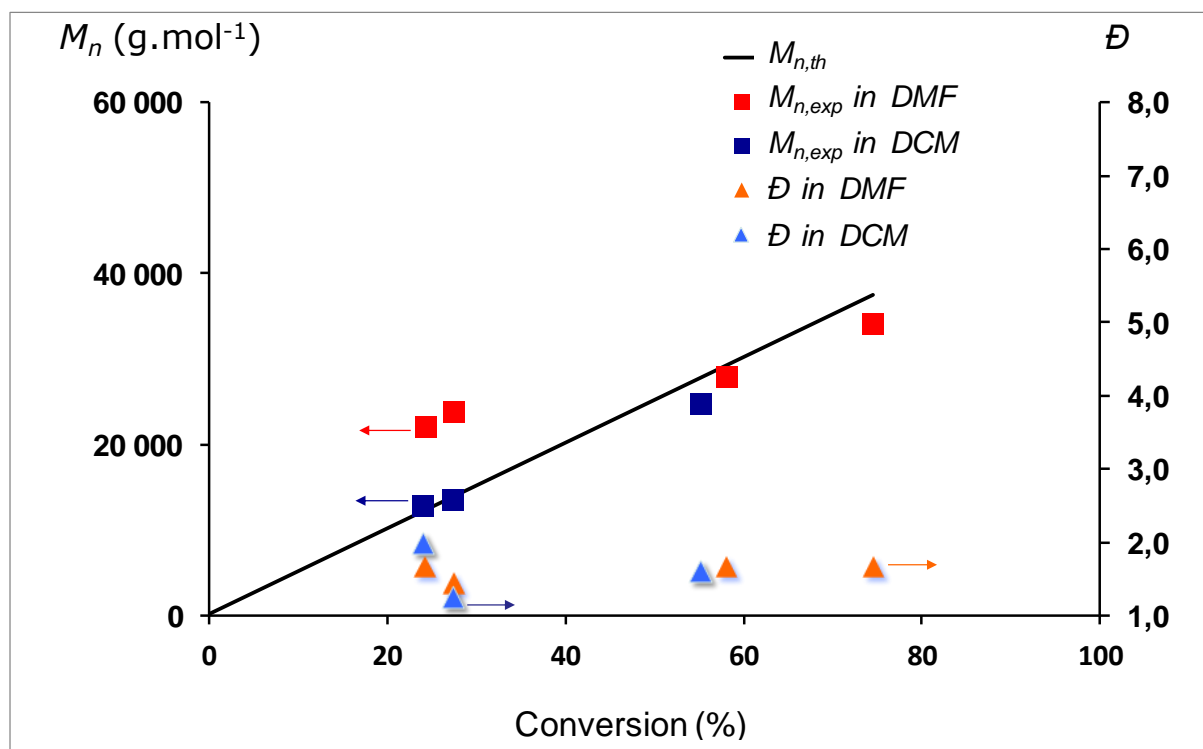
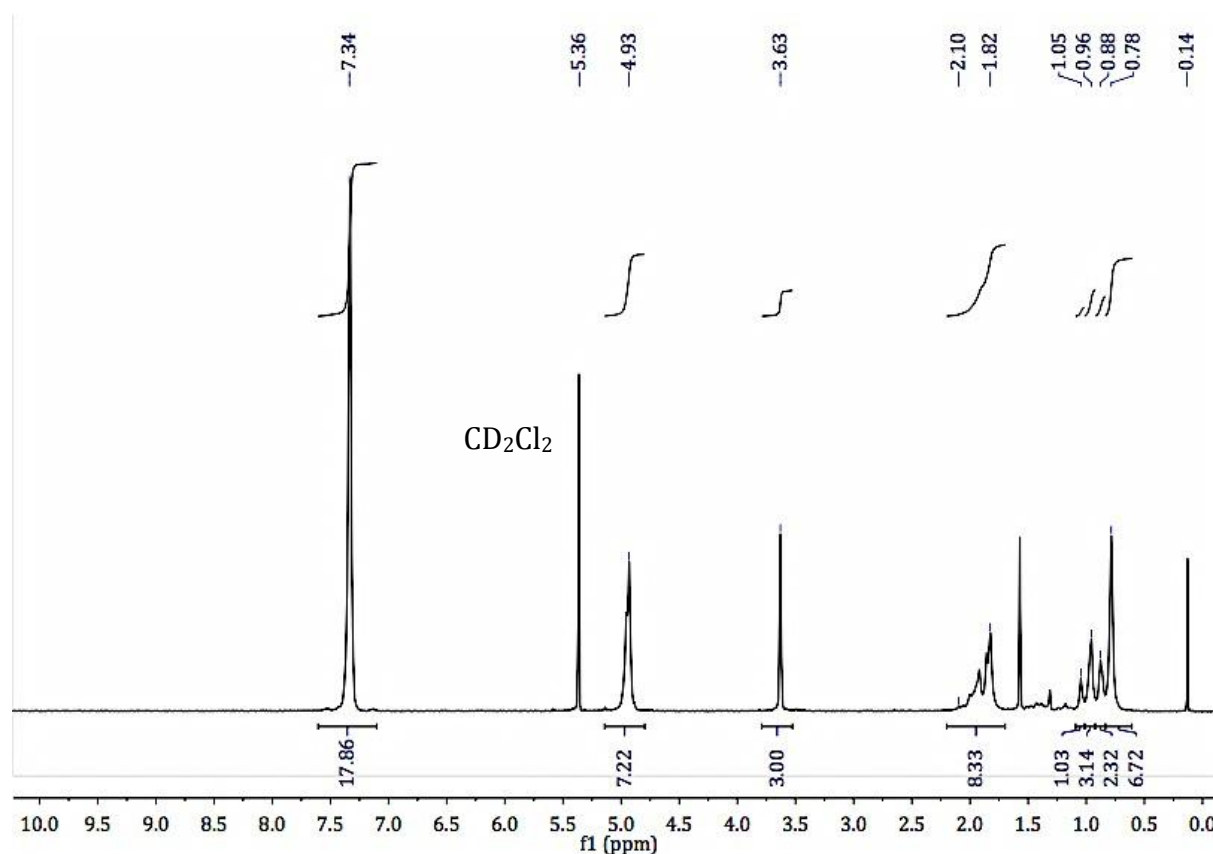


Figure 17-SI-14. Dependence of molecular weights, M_n (■) and molecular weight distributions, M_w/M_n (Δ), on the monomer conversion for the ATRP of MMA in DMF or in DCM at rt. $[\text{Au}_2]/\text{EBPA}/\text{MMA}$, 0.0125/1/500.

D. General chain extension procedure

In a schlenk charged with the precipitated PMMA ($M_{n,exp} = 14.2$ kg/mol, $M_w/M_n = 1.48$, 50 mg, 1 eq.) dissolved in DMF (1.5 mL) and BnMA 1.2 M in DMF (298 μ L, 500 eq.). After covering the schlenk with aluminum foil, a solution of complex **1** $4.3 \cdot 10^{-3}$ M in DMF (11 μ L, 0.0125 eq.) was added. The reaction mixture was degassed by freeze-pump-throw three times. After 14 h stirred in Rayonet under light exposure ($\lambda = 350$ nm), the reaction mixture was covered with aluminum foil and transferred via syringe to a round bottom flask containing a cold mixture of methanol (53 mL). The white precipitate was filtered over filter paper under water pump vacuum and collected with DCM to give the desired product. Aliquots from the reaction mixture were removed to give the conversion of BnMA using gravimetric method and analyzed by SEC to give polymer characteristic (M_n , M_w , M_w/M_n). $M_{n,exp} = 37.4$ kg/mol, $M_w/M_n = 2.0$. ^1H NMR (300 MHz, CD_2Cl_2): δ 7.26 (s, 17.9H), 4.93 (bs, 7.22), 3.63 (s, 3H), 2.10-1.82 (m, 8.33), 1.05 (m, 1.03), 0.96 (m, 3.14H), 0.88 (m, 2.32H), 0.78 (s, 6.72) ppm. IR (neat): ν 2961, 1722, 1453, 1388, 1236, 1141, 966, 912, 751, 696 cm^{-1} .

E. NMR spectrum



F. Mass Spectrometry study on PMMA

To further support the livingness character of our system, the nature of the end group of the synthesized PMMA polymer was determined by MALDI-TOF (Figure 19-SI-S16) and ESI-TOF (Figure 20-SI-S17) mass spectrometry analysis of a crude mixture of low molecular weight polymers obtained after stopping the process at 25% conversion. Several conditions for MALDI analysis were tested using dithranol, 2,5-dihydroxybenzoic acid (DHB) or *trans*-2-[3-(4-tert-butylphenyl)-2-methyl-2-propenylidene] malononitrile (DCTB) as a matrix and NaI or LiCl as a cationizing agent. In all cases, the same mass spectrum was obtained and confirmed that the repeat unit corresponds to the monomer unit without mass loss (100.1 m/z). The major population was identified as the Na⁺-ionized polymer showing a lactone chain end. Previously evidenced in the literature,[4] this motif originates from lactonization of the bromide during the mass spectral analysis. A minor population can be assigned to the Na⁺-ionized polymer formed after debromination. Another resulting from a reductive debromination can also be observed exclusively in the ESI spectrum. However, no trace of polymer with bromo chain end group was detected. By comparison, the same type of polymers with low molecular weight prepared by using the Hawker's conditions with Ir(ppy)₃ as catalyst[5] and analyzed MALDI-TOF MS (Figure 21-SI-S17) and ESI-TOF MS (Figure 22-SI-S18) provided the same results.

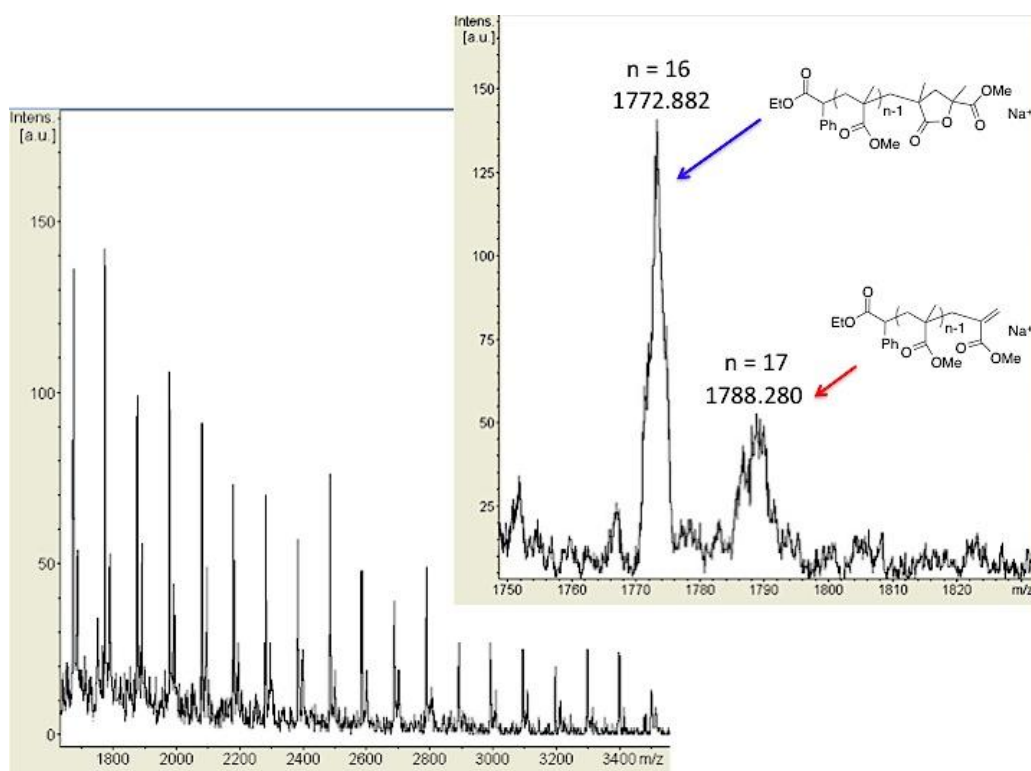


Figure 19-SI-16. MALDI-TOF MS of the crude after MMA polymerization using gold catalyst (1).

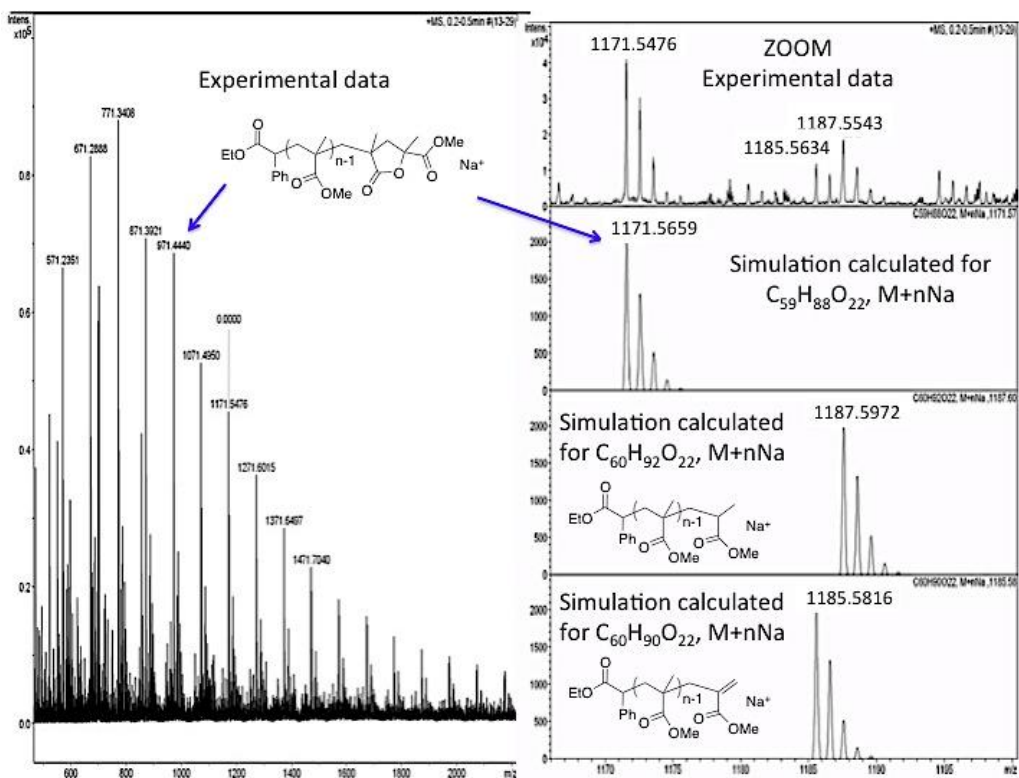


Figure 20-SI-17. ESI-TOF MS of the crude after MMA polymerization using gold catalyst (1).

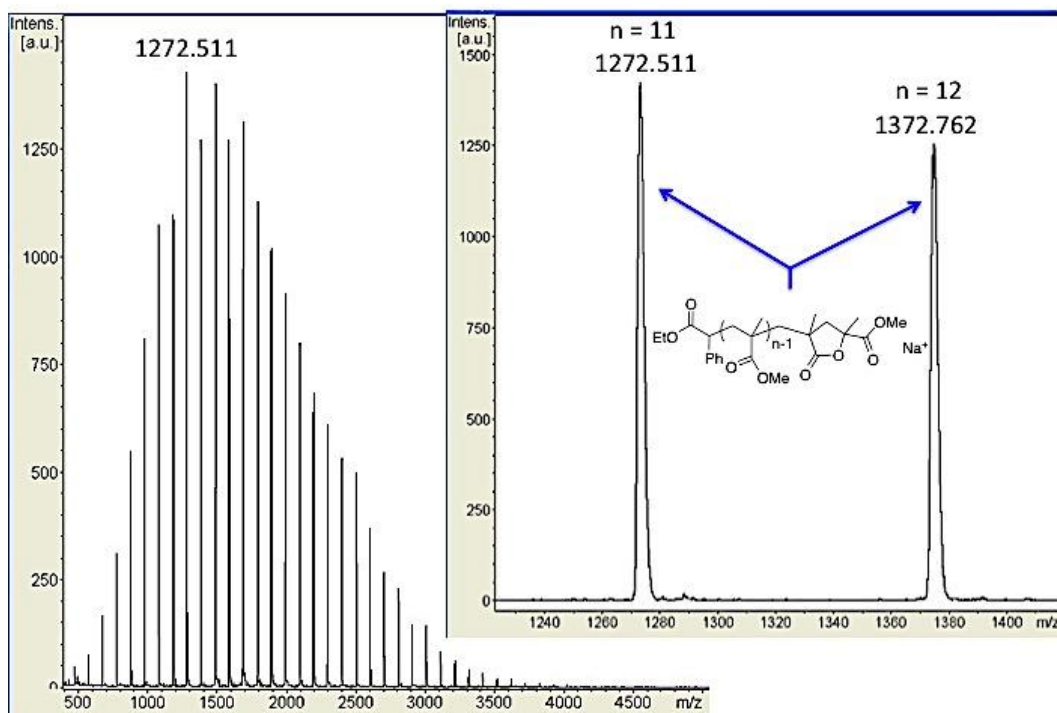


Figure 21-SI-17. MALDI-TOF MS of the crude after MMA polymerization using $Ir(ppp)_3$.

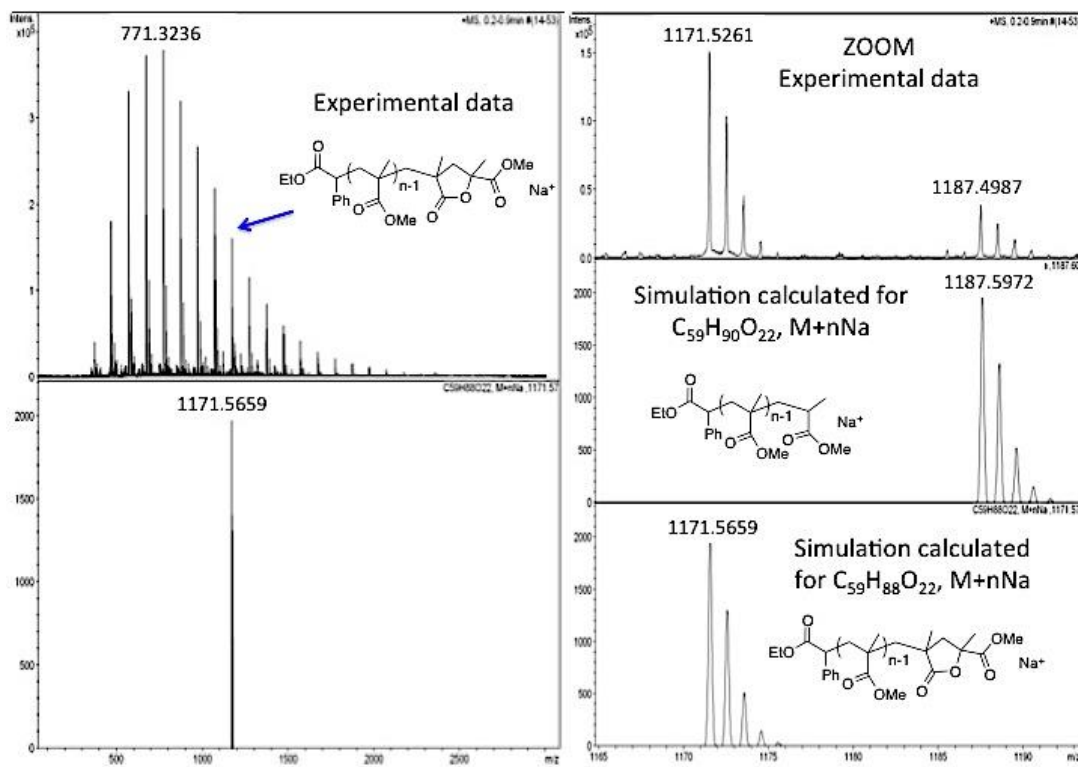


Figure 22-SI-18. ESI-TOF MS of the crude after MMA polymerization using Ir(ppy)₃.

G. Atom Transfer Radical Addition (ATRA) experiment

We investigated the ability of gold complex **1** to catalyse atom-transfer radical addition (ATRA) reactions. First, we tested the reaction between EBPA and 1-octene in the presence of 1 mol% of **1** but no ATRA product was formed after 24 h reaction. Thus, we decided to test the conditions developed by Boyer *et al.*[6] with allyl alcohol as olefin and Ir(ppy)₃ as catalyst. Comparison of the NMR spectra of the crude after 4 h reaction with the reaction performed with gold complex **1** under the same conditions shows the same spectral data which are in accordance with those reported in the literature[6] (Figures 23 and 24-SI-19). These results indicate the formation of the desired product and confirm that Au₂-complex **1** is able to catalyse ATRA reaction between EBPA and allyl alcohol.

ATRA experiment was performed according to the Boyer's procedure.[6] The complex **1** (3.26 mg, 0.0025 mmol) was dissolved in DMSO-*d*₆ (1.0 mL) and degassed by N₂ bubbling for 30 min. In the dark, ethyl α-bromophenylacetate (87.4 μL, 0.5 mmol) and allyl alcohol (17 μL, 0.25 mmol) were added. After 4 h stirred in Rayonet under light exposure (λ = 350 nm), the reaction mixture was stopped. Characteristic signals of the ATRA compound. ¹H NMR (300 MHz, CD₂Cl₂): δ 7.22-7.64 (m, 5H), 4.28-4.45 (m, 1H), 4.00-4.22 (m, 2H), 3.53-3.80 (m, 1H), 3.30-3.44 (m, 2H).

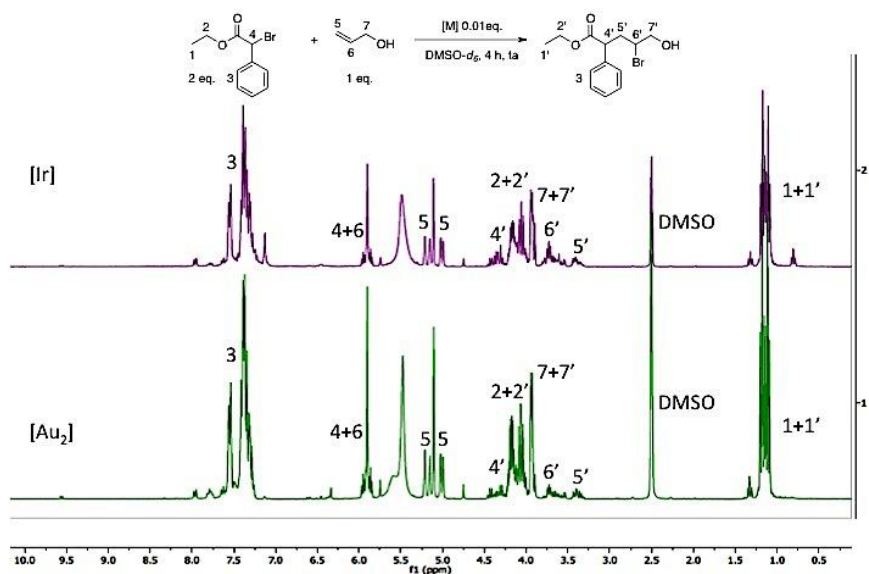


Figure 23-SI-19. ^1H NMR spectra of the reaction mixture of ethyl- α -bromophenylacetate to allyl alcohol using 1 mol% of $\text{Ir}(\text{ppy})_3$ (purple line) at 470 nm and $[\text{Au}_2]$ (green line) at 350 nm in $\text{DMSO-}d_6$.

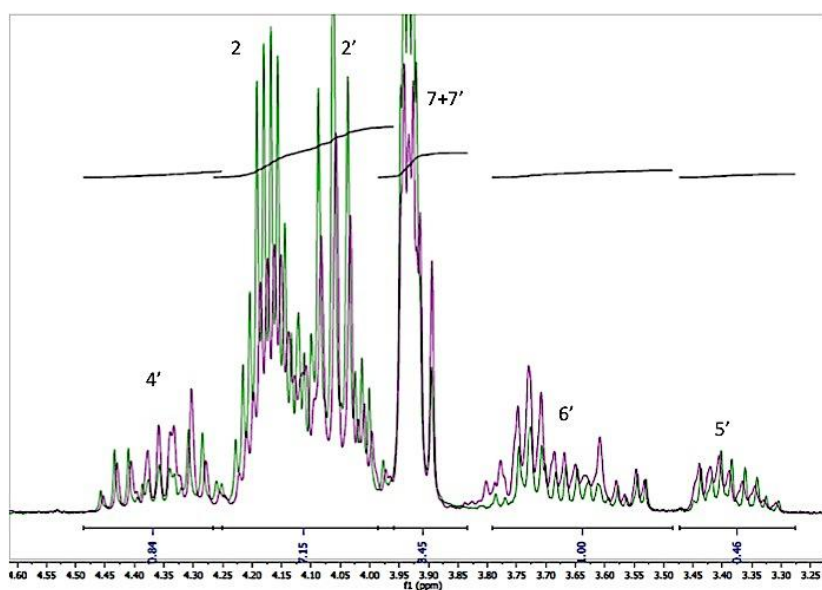


Figure 24-SI-19. Zoom of the superimposed ^1H NMR spectra.

IV. Photopolymerization in laminate

A. General photopolymerization procedure

In laminate: TMPTA was irradiated in laminate (the formulation is sandwiched between two polypropylene films). The evolution of the acrylate content is continuously followed by real time FTIR spectroscopy (FTIR NEXUS 870) at $\sim 1620\text{ cm}^{-1}$. A LED 405 nm ($I_0 \approx 110\text{ mW cm}^{-2}$) was used as irradiation source.

1. Luminescence spectrum of the formulation after irradiation

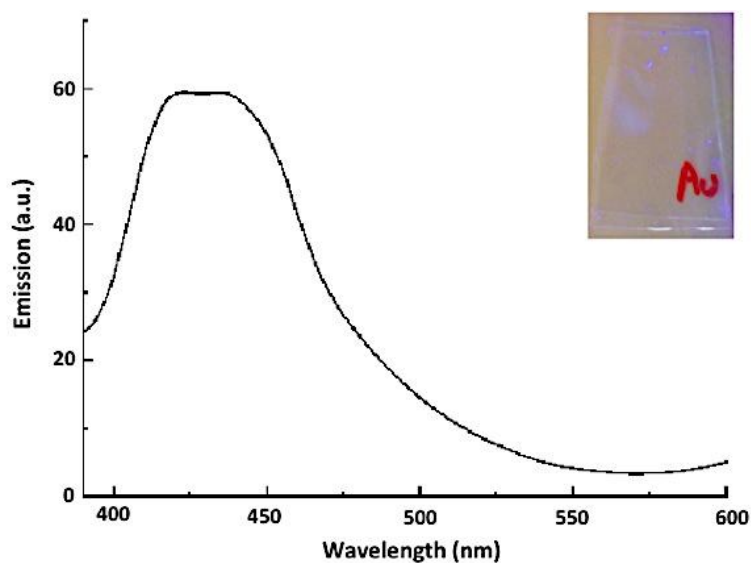


Figure 25-SI-20. Film phosphorescence spectrum, recorded with an excitation at 340 nm. Formulation of $[\text{Au}_2]/\text{TMPTA}/\text{EBPA}$ (0.0125/100/1 mol/mol).

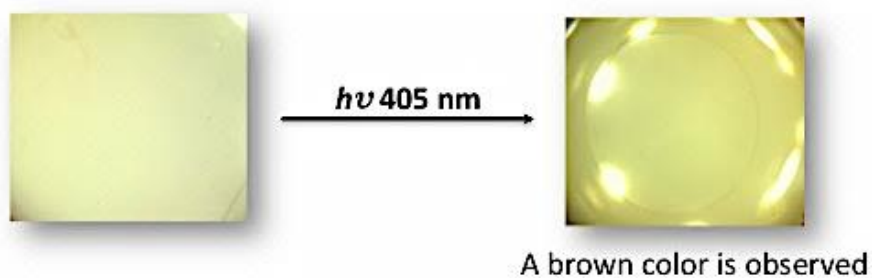


Figure 26-SI-20. Film absorption spectrum. Formulation of $[\text{Au}_2]/\text{TMPTA}/\text{EBPA}$ (0.0125/100/1 mol/mol).

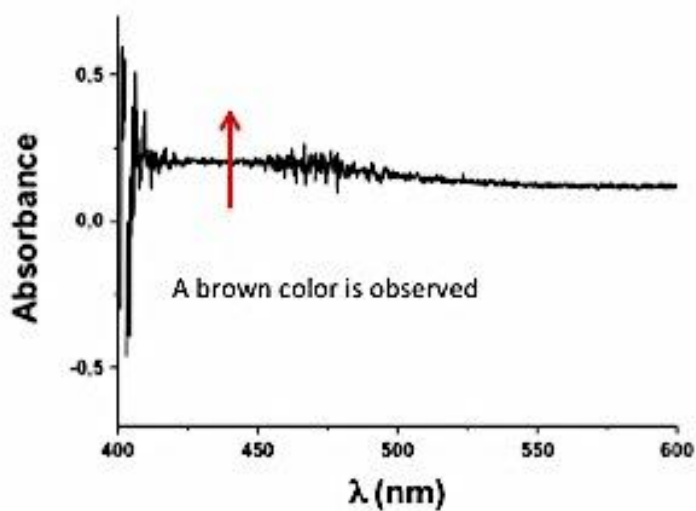


Figure 27-SI-20. Film colorimetry analysis after 30 min of irradiation under LED bulbs (405 nm). Formulation of $[\text{Au}_2]/\text{TMPTA}/\text{EBPA}$ (0.0125/100/1 mol/mol).



Figure 28-SI-21. Gold + EBPA colorimetry analysis after 10 s of irradiation under Xe-Hg. Formulation of $[Au_2] = 3 \cdot 10^{-4}$ M, $[EBPA] = 6.6 \cdot 10^{-3}$ M.

2. Transmission Electron Microscopy (TEM)

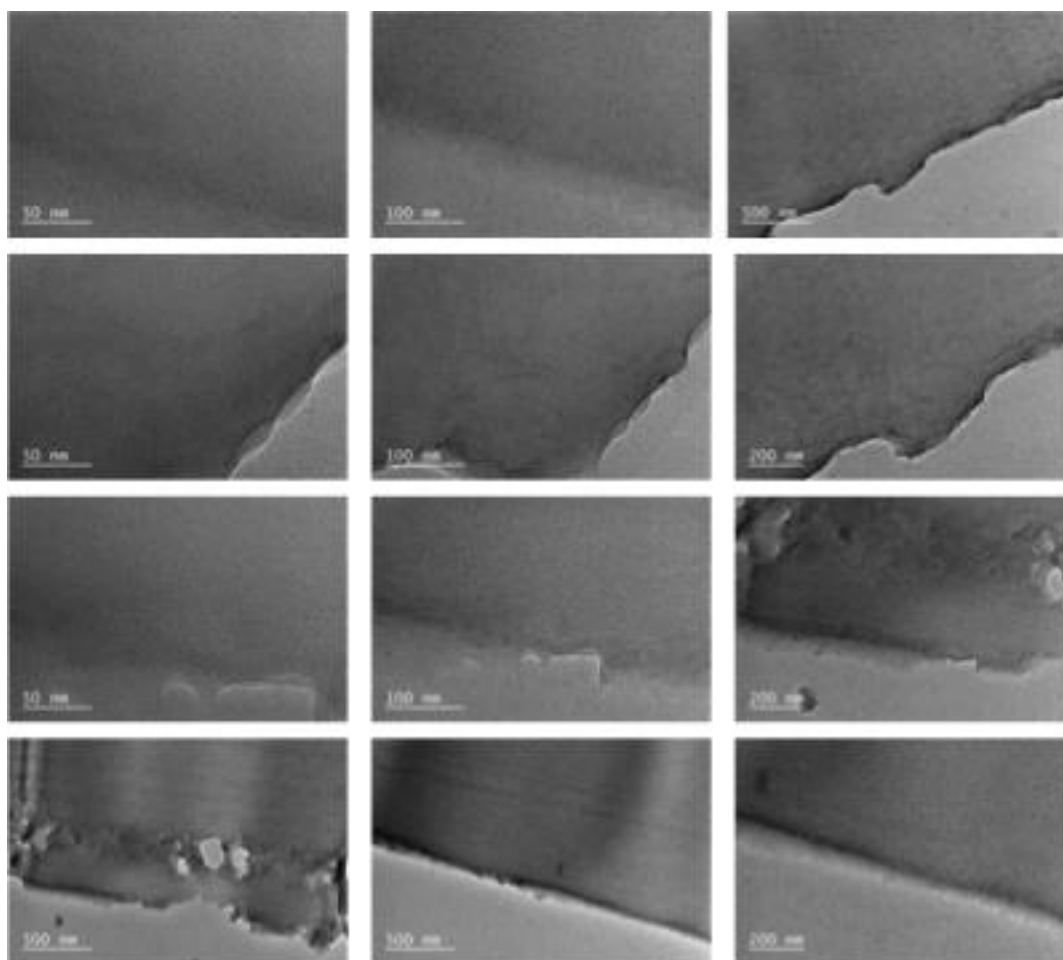
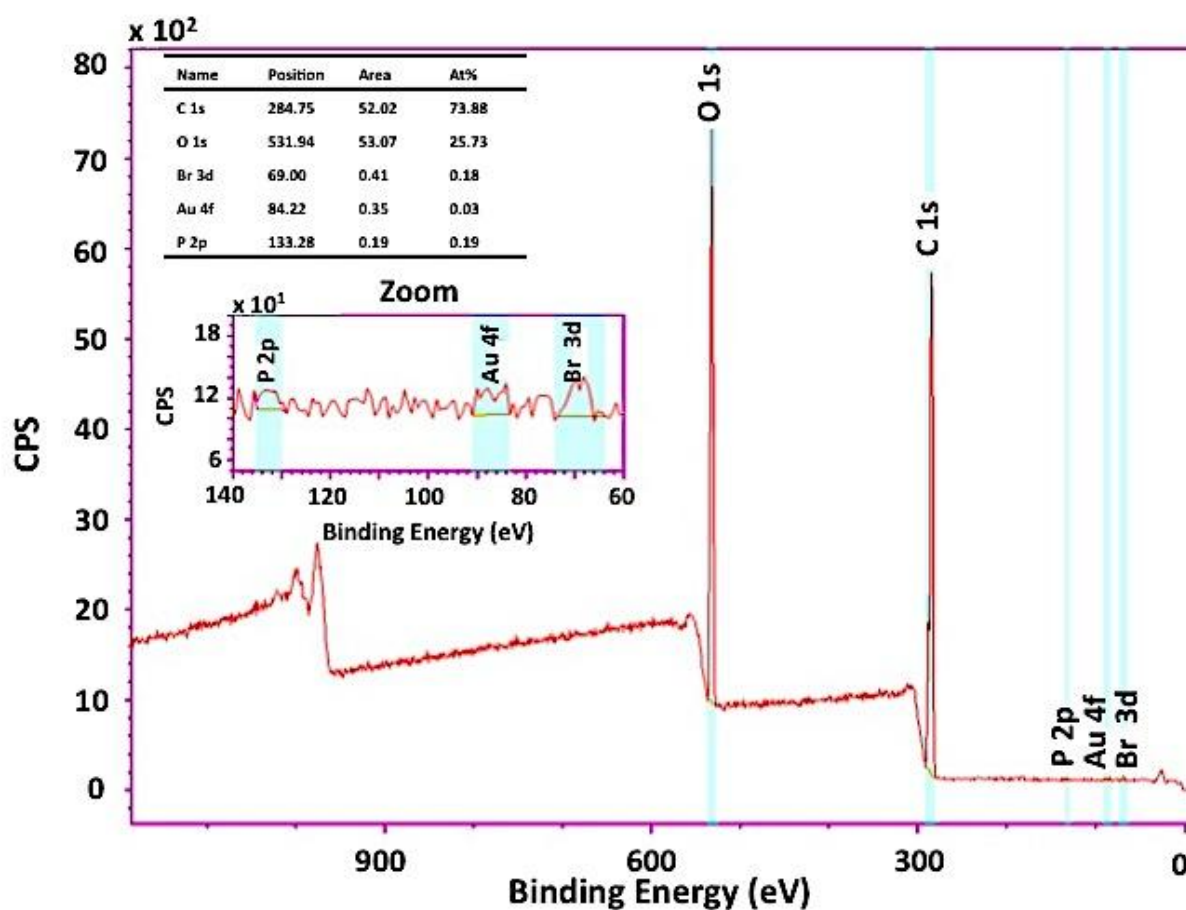


Figure 29-SI-21. TEM pictures. Evidence of absence of $[Au]$ nanoparticles after 3 min of irradiation with blue LED 405 nm in laminate. Formulation of $[Au_2]/TMPTA/EBPA$ (0.0125/100/1 mol/mol).

3. X-ray Photoelectron Spectroscopy (XPS)

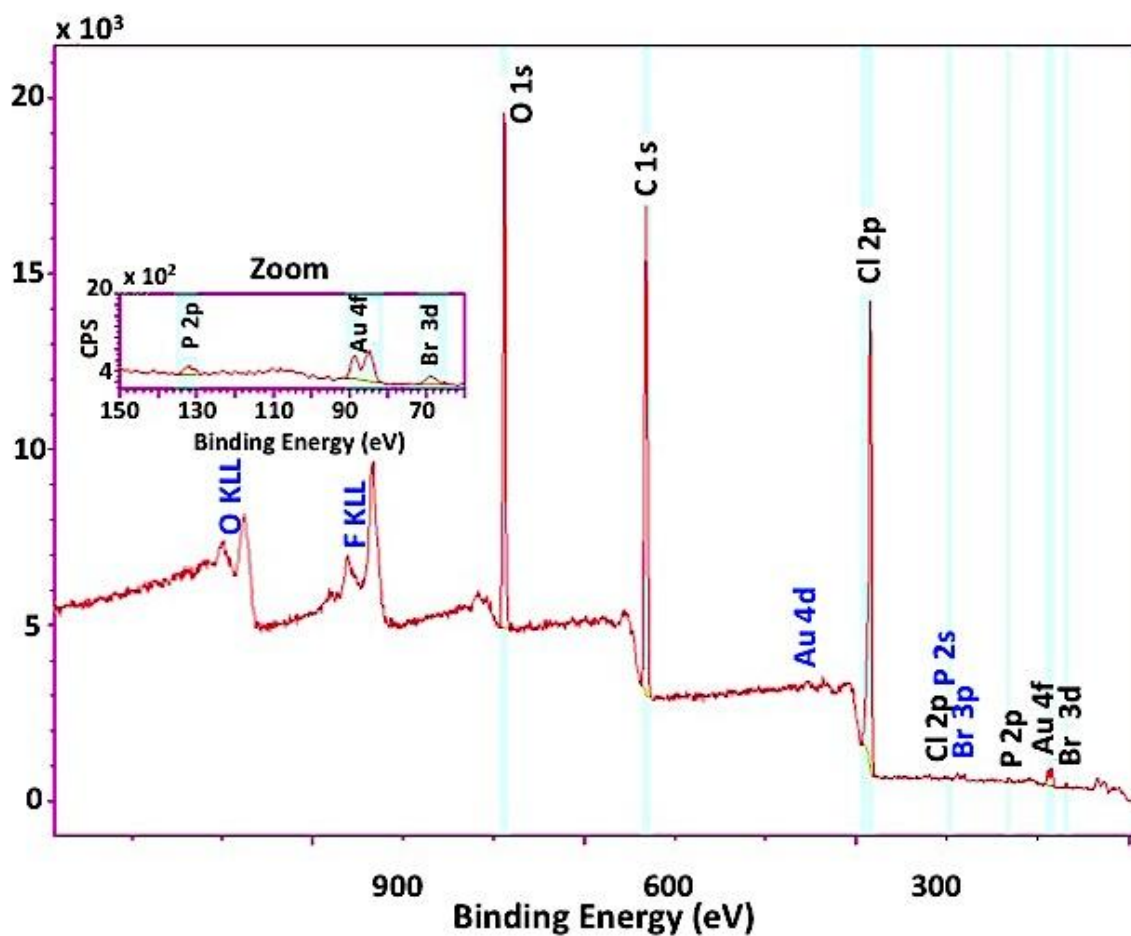
1st layer : Formulation of TMPTA 5/[Au₂]/EBPA: 1/0.01/0.03 mol/mol. Irradiated for 3 minutes with blue LED 405 nm in laminate.

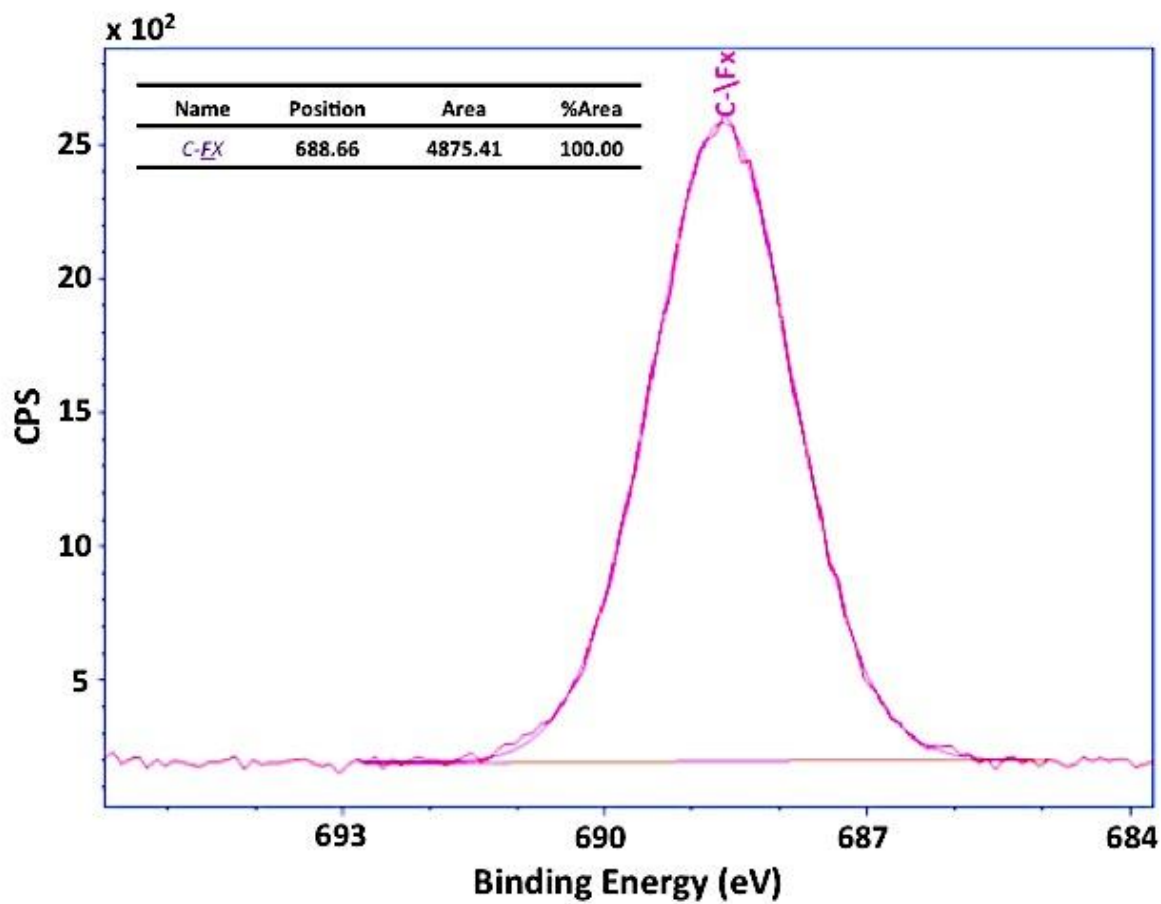
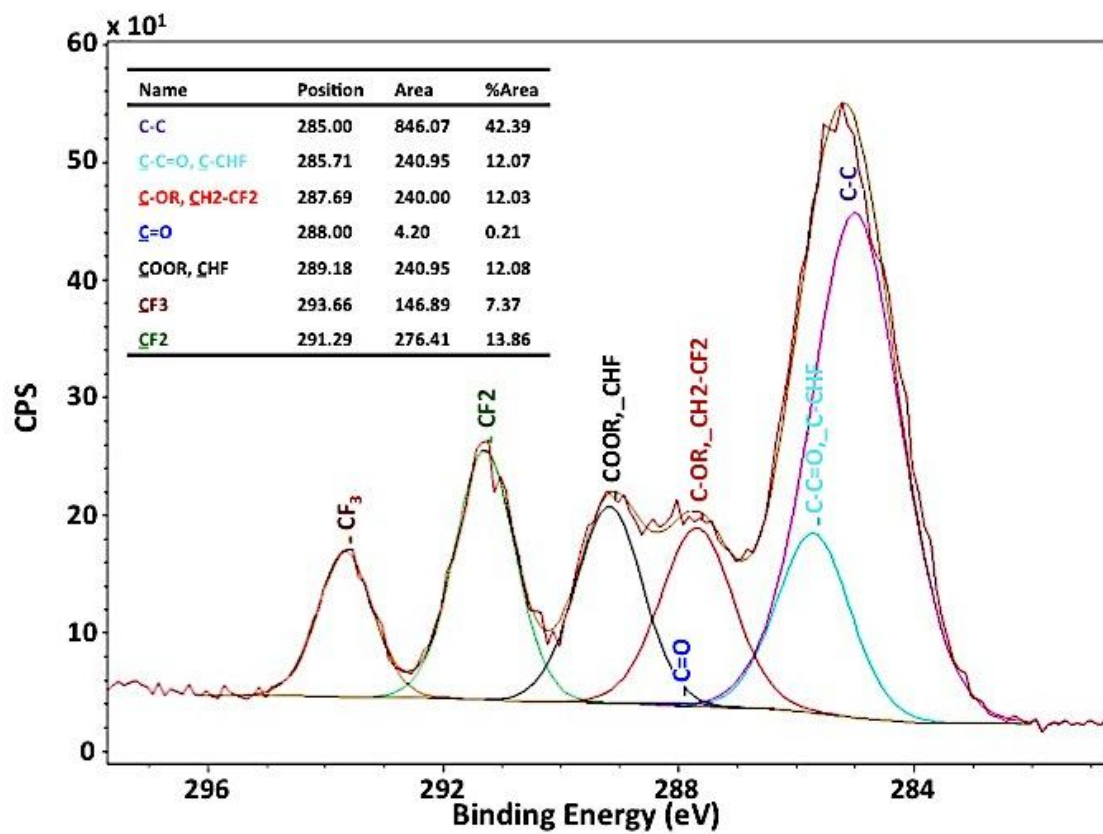
Name	Position	Area	Atomic%	Weight%
C 1s	285,00	147,71	74,97	68,92
O 1s	531,75	49,23	24,99	30,60
Au 4f	84,75	0,04	0,02	0,32
Br 3d	69,75	0,05	0,03	0,16



2nd layer : Copolymerization using a fluorinated monomer (HFBA, **6**) after irradiated with Xe-Hg lamp for 10 minutes in laminate.

Name	Position	Area	Atomic%	Weight%
C 1s	285,00	127,04	63,90	53,43
O 1s	531,75	42,06	21,15	23,56
F 1s	688,50	27,92	14,04	18,57
Au 4f	84,75	0,31	0,15	2,12
Br 3d	69,00	0,37	0,19	1,04
P 2p	132,00	0,83	0,42	0,90
Cl 2p	199,50	0,29	0,15	0,36





References

- [1] a) N. M. Atherton, M. J. Davies, B. C. Gilbert, P. Tordo. Spin-Trapping: Recent Developments and Applications. In *Electron Paramagnetic Resonance: Volume 16*, B. C. Gilbert, N. M. Atherton, M. J. Davies eds., The Royal Society of Chemistry Cambridge, U.K., **1998**, *16*, pp. 116; b) J. Lalevée, F. Dumur, C. R. Mayer, D. Gigmes, G. Nasr, M. A. Tehfe, S. Telitel, F. Morlet-Savary, B. Graff, J. P. Fouassier, *Macromolecules*, 2012, **45**, 4134.
- [2] a) J. Lalevée, N. Blanchard, C. Fries, M.-A. Tehfe, F. Morlet-Savary, J.P. Fouassier, *Polym. Chem.*, 2011, **2**, 1077; b) S. Telitel, J. Lalevée, N. Blanchard, T. Kavalli, M.-A. Tehfe, F. Morlet-Savary, B. Graff, J.P. Fouassier, *Macromolecules*, 2012, **45**, 6864; c) M.-A. Tehfe, J. Lalevée, F. Morlet-Savary, B. Graff, N. Blanchard, J.P. Fouassier, *ACS Macro Lett.*, 2012, **1**, 198.
- [3] G. Revol, T. McCallum, M. Morin, F. Gagosz, L. Barriault, *Angew. Chem. Int. Ed.*, 2013, **52**, 13342.
- [4] a) N. K. Singha, S. Rimmer, B. Klumperman, *Eur. Polym. J.*, 2004, **40**, 159; b) A. T. Jackson, A. Bunn, I. M. Priestnall, C. D. Borman, D. J. Irvine, *Polymer*, 2006, **46**, 1044.
- [5] B. P. Fors, C. J. Hawker, *Angew. Chem. Int. Ed.*, 2012, **51**, 8850.
- [6] J. Xu, A. Atme, A. F. Marques Martins, K. Jung, C. Boyer, *Polym. Chem.*, 2014, **5**, 3321.